Genetic and Phenotypic Analysis of Alleles of the Drosophila Chromosomal JIL-1 Kinase Reveals a Functional Requirement at Multiple Developmental Stages

Weiguo Zhang, Ye Jin, Yun Ji, Jack Girton, Jørgen Johansen and Kristen M. Johansen[1]

Department of Biochemistry, Biophysics, and Molecular Biology, Iowa State University, Ames, Iowa 50011

Manuscript received April 12, 2003
Accepted for publication July 31, 2003

ABSTRACT

In this study we provide a cytological and genetic characterization of the *JIL-1* locus in Drosophila. JIL-1 is an essential chromosomal tandem kinase and in *JIL-1* null animals chromatin structure is severely perturbed. Using a range of *JIL-1* hypomorphic mutations, we show that they form an allelic series. JIL-1 has a strong maternal effect and JIL-1 activity is required at all stages of development, including embryonic, larval, and pupal stages. Furthermore, we identified a new allele of *JIL-1*, *JIL-1*^{h9}, that encodes a truncated protein missing COOH-terminal sequences. Remarkably, the truncated JIL-1 protein can partially restore viability without rescuing the defects in polytene chromosome organization. This suggests that sequences within this region of JIL-1 play an important role in establishing and/or maintaining normal chromatin structure. By analyzing the effects of *JIL-1* mutations we provide evidence that JIL-1 function is necessary for the normal progression of several developmental processes at different developmental stages such as oogenesis and segment specification. We propose that JIL-1 may exert such effects by a general regulation of chromatin structure affecting gene expression.

RECENTLY we identified a tandem kinase, JIL-1, that mediates histone H3 phosphorylation on serine 10 (H3 Ser10) and is required for normal chromosome morphology in both males and females in Drosophila (Jin *et al.* 1999; Wang *et al.* 2001). The JIL-1 kinase is an essential protein that associates with all chromosomes throughout the cell cycle (Jin *et al.* 1999). However, JIL-1 is found at twofold higher levels on the male X chromosome and associates with the male-specific lethal (MSL) dosage compensation complex (Jin *et al.* 2000). The MSL complex is required for the necessary hyper-transcription of genes on the male X chromosome for dosage compensation in flies (reviewed in Meller and Kuroda 2002). This enhanced transcription is thought to arise from MSL-complex-induced histone H4 acetylation generating a more open chromatin structure (Smith *et al.* 2000). The increased histone H3 Ser10 phosphorylation levels that JIL-1 promotes on the male X may also play a role in maintaining its more open and active chromatin structure (Jin *et al.* 2000; Wang *et al.* 2001). In mutant animals carrying *JIL-1* null or hypomorphic alleles leading to decreased levels of JIL-1 protein, the euchromatic regions of all larval salivary gland polytene chromosomes are severely reduced and the chromosome arms are condensed, although the male X chromosome is the most severely perturbed (Wang *et al.* 2001). Thus, JIL-1 plays an important role in the establishment or maintenance of chromatin structure of both autosomes and sex chromosomes.

Furthermore, we have recently demonstrated that JIL-1 interacts with a novel isoform, LOLA zf5, from the *lola* locus of zinc-finger-containing transcription factors (Zhang *et al.* 2003). The expression of LOLA zf5 is restricted to early embryogenesis (Zhang *et al.* 2003) and consequently JIL-1's interaction with LOLA zf5 is developmentally regulated. It is therefore likely that JIL-1 plays a role in several different molecular complexes regulating chromatin structure and gene expression at different times in development. However, the requirement for JIL-1 function during development has not been thoroughly characterized and it is not clear at what stages JIL-1 is needed. In this study we have taken a genetic approach to characterize the requirement for JIL-1 at different stages by assessing the effects of an allelic series of hypomorphic and null alleles on viability and development. We molecularly define the lesions present in previously reported JIL-1 alleles and we characterize a new allele that reveals an important functional requirement for JIL-1 COOH-terminal sequences. These results show that JIL-1 has a strong maternal effect and is necessary for viability throughout development. In addition, homeotic transformation phenotypes observed in JIL-1 mutant animals suggest that JIL-1 may influence gene expression of homeotic genes in a manner similar to that of trithorax group genes.

[1]*Corresponding author:* Department of Biochemistry, Biophysics, and Molecular Biology, 3154 Molecular Biology Bldg., Iowa State University, Ames, IA 50011. E-mail: kristen@iastate.edu

MATERIALS AND METHODS

Drosophila stocks: Fly stocks were maintained according to standard protocols (Roberts 1998). Oregon-R was used for wild-type preparations. Balancer chromosomes and mutant alleles are described in Lindsley and Zimm (1992). Strains used for deletion mapping experiments contained deficiencies uncovering the 68A–C region and included *Df(3L)vin2/TM3*, *Df(3L)vin3 e^{1}/TM3 ry**, *Df(3L)vin4 e^{1}/TM3 ry**, *Df(3L)vin5 e^{1}/TM3 Sb^{1} Ser^{1}*, and *y^{1}; Df(3L)lxd6/TM3 y^{+} Sb^{1} e^{1} Ser^{1}* (from the Bloomington Stock Center), *Df(3L)lxd8 cur/TM3 Sb* and *Df(3L)h9/TM3* (gift from V. Finnerty), and *Df(3L)h76 red/TM3* (kindly provided by A. Hilliker). Five lethal mutants previously mapped to the 68A4–5 region were used in rescue experiments: *l(3)l-58 e^{s} sr ca/TM3 Sb Ser*, *l(3)EMSl-1 sr e^{s} ca/TM3 Sb Ser*, and *l(3)l-55 sr e^{s} ca/TM3 Sb Ser* were from A. Hilliker; *mre l(3)517/TM1 M$_{e}$* (= *l(3)68Ag*) was from A. Shearn; and *P{ry$^{+t7.2}$ = PZ}l(3)01239^{01239} ry^{506}/TM3, ry^{RK}Sb^{1} Ser^{1}* was from the Bloomington Stock Center where we also obtained the *brm^{2} trx^{E2} ca^{1}/TM6B, Tb^{1} ca^{1}* line. Genetic interaction assays were performed using *y,w* ; +/+; +/+ and *brm^{2} trx^{E2} ca^{1}/TM3 Tb Hu e*. *JIL-1^{z2}*, *JIL-1^{z60}*, and *JIL-1$^{EP(3)3657}$* are described in Wang *et al.* (2001). *JIL-1^{z28}* is a less severe, hypomorphic *JIL-1* imprecise excision allele generated during that study but not previously described. *JIL-1^{Scim}* is described in Dobie *et al.* (2001) and was the generous gift of K. Dobie and G. Karpen.

Polytene chromosome *in situ* hybridization: *In situ* hybridization was performed essentially as described in Roberts (1998). Salivary glands from late third instar larvae were dissected in 0.7% saline solution, fixed in 45% acetic acid, and squashed on clean slides in 20 μl lactic and acetic acid solution (1:2:3 parts lactic acid:H_2O:acetic acid). Slides with good chromosome spreads were then immersed in liquid nitrogen, coverslips were removed, and chromosomes were denatured in 0.2 n NaOH. Preparations were hybridized with digoxigenin-labeled *JIL-1* cDNA prepared using the DNA labeling kit from Boehringer Mannheim (Indianapolis) according to the manufacturer's instructions. After hybridization overnight at 42°, polytene chromosomes were washed sequentially with 2× SSC, PBS, and AP buffer (100 mm Tris, 100 mm NaCl, 5 mm $MgCl_2$, pH 9.5) at room temperature and incubated with alkaline phosphatase-conjugated antidigoxigenin antibody in Blotto (5% dry milk in PBS) for 2 hr. The hybridization signal was detected by incubating slides in color reaction buffer (57 μl nitrotetrazolium blue, 52 μl 5-bromo-4-chloro-3-indolyl phosphate in 15 ml AP buffer) for 1–2 hr and observed by phase-contrast microscopy on a Zeiss Axioskop.

Molecular mapping of *JIL-1* imprecise excision mutants: The *JIL-1^{z2}*, *JIL-1^{z60}*, and *JIL-1^{z28}* alleles were generated by mobilizing the Enhancer *P* (EP) transposon (Rørth *et al.* 1998) inserted in the *JIL-1* locus in the *JIL-1$^{EP(3)3657}$* line (Wang *et al.* 2001). Likewise, *Df(3L)h9* was generated by imprecise *P*-element excision (Campbell *et al.* 1986). DNA was isolated from single homozygous mutant larvae or embryos and PCR reactions were performed as previously described (Preston and Engels 1996; Wang *et al.* 2001). PCR-based chromosome walking was used to narrow down the *Df(3L)h9* deficiency breakpoints into a small region followed by PCR and direct sequencing. PCR primers were designed in such a way that each round of PCR located the breakpoints in a chromosome region that was half the length of that in the previous round. Primer sequences used in mutant mapping are available upon request.

Immunoblot analysis: Protein extracts were prepared from staged wild-type embryos, larvae, pupae, or adults that were homogenized in immunoprecipitation buffer (20 mm Tris-HCl, 150 mm NaCl, 10 mm EDTA, 1 mm EGTA, 0.2% Triton X-100, 0.2% NP-40, 2 mm Na_3VO_4, pH 8.0) with the added protease inhibitors 1.5 μg/ml aprotinin and 1 mm phenylmethylsulfonyl fluoride (Sigma, St. Louis). Homozygous mutant larvae were identified by absence of the *Tubby* marker. Proteins were boiled in SDS-PAGE buffer, separated on 10% SDS-PAGE gels, transferred to nitrocellulose, blocked in 5% Blotto containing 0.2% Tween-20, and incubated with anti-JIL-1 or anti-α-tubulin antibody overnight. Blots were then washed three times for 10 min in TBST (0.9% NaCl, 100 mm Tris-HCl, pH 7.5, 0.2% Tween-20), incubated with horseradish peroxidase-conjugated goat anti-rabbit or anti-mouse secondary antibody (1:3000; Bio-Rad, Richmond, CA) for 1 hr at room temperature, washed in TBST, and the antibody signal was detected with the enhanced chemiluminescence kit according to the manufacturer's instructions (Amersham Pharmacia). For quantification of immunolabeling, exposures of immunoblots on Biomax ML film (Kodak) were scanned with an Arcus II (AGFA) flatbed scanner and the digital images were analyzed using the NIH-Image software. In these images the grayscale was adjusted such that only a few pixels in the wild-type lanes were saturated. The area of each band was traced using the outline tool and the average pixel value was determined. Levels in *JIL-1* mutant larvae were determined as a percentage relative to the level determined for wild-type control larvae.

Staining of polytene chromosomes: Polytene chromosome preparation and staining was essentially as in Wang *et al.* (2001). Polytene chromosomes from late third instar larva were first fixed in 3.7% paraformaldehyde for 30 sec, refixed in a solution of 50% glacial acetic acid and 3.7% paraformaldehyde for 2–5 min, and squashed. Preparations with good spreads were stained with 0.2 μg/ml Hoechst 33258 (Molecular Probes, Eugene, OR) for 5 min. After a final brief rinse with distilled water, the preparations were mounted in 90% glycerol containing 0.5% *n*-propyl gallate. The chromosomes were examined under epifluorescence optics using a Zeiss Axioskop microscope and the images were captured and digitized with a high-resolution Spot CCD camera (Diagnostic Instruments). Subsequent image processing was carried out using Adobe Photoshop, version 7.0.

Ovary dissection and staining: Wild-type or *JIL-1* mutant females were aged for 3–4 days before dissection. For comparison of ovary sizes, dissected ovaries were placed in a drop of PBS (0.9% NaCl, 14 mm Na_2HPO_4, 6 mm NaH_2PO_4, pH 7.3) under an Olympus dissection microscope, and images were taken with a Paultek cooled CCD camera and analyzed using NIH-Image software. The area of each ovary was traced using the outline tool and determined in square millimeters. Fixed ovaries were stained with Hoechst 33258 (Molecular Probes) for 10 min followed by PBS wash for 10 min to visualize DNA (Sullivan *et al.* 2000). Manually separated ovarioles were mounted in 90% glycerol containing 0.5% *n*-propyl gallate. Confocal microscopy was performed with a Leica confocal TCS NT microscope system equipped with an Argon-UV laser and appropriate filter set.

Adult cuticle preparation: Preparation of adult cuticles was performed as previously described (Girton and Jeon 1994). Briefly, adult males or females were preserved in 70% ethanol. Individuals were heated at 92° in 1 n KOH for 5–10 min to remove internal tissues and then dehydrated in ethanol. Adult abdomens were cut along their dorsal midline with a razor blade and mounted in a drop of euparol. After mounting, each specimen was dried and flattened on a slide-warming tray under weights for 24 hr. Brightfield images of the preparations were obtained using a Zeiss Axioskop and a digital Spot camera.

RESULTS

Cytological and genetic characterization of the 68A region containing the *JIL-1* locus: By hybridizing digoxi-

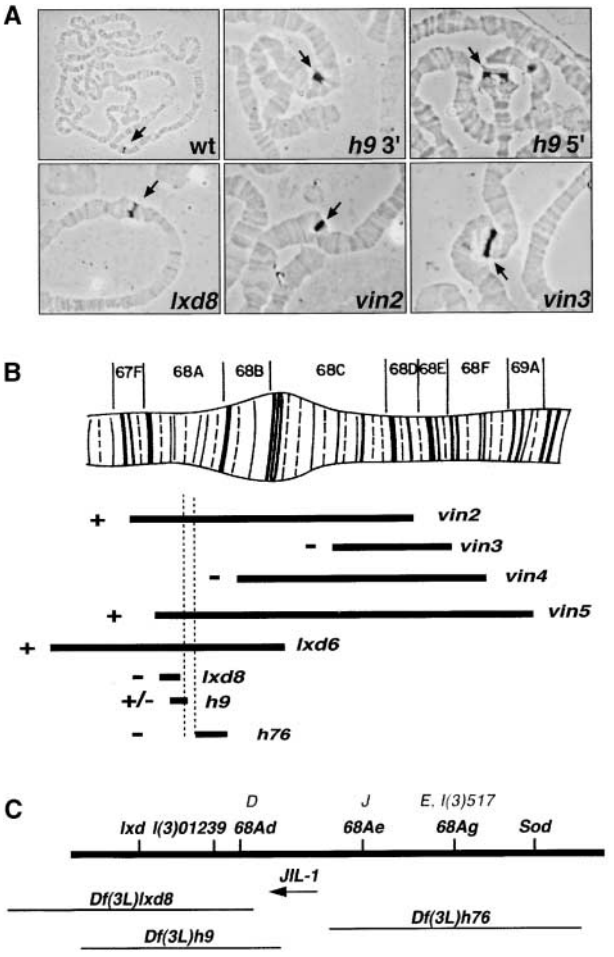

FIGURE 1.—Cytological and genetic mapping of the *JIL-1* locus. (A) *In situ* hybridization using digoxigenin-labeled *JIL-1* cDNA probes was used to map the *JIL-1* locus to region 68A on wild-type (wt) polytene chromosomes. Hybridization was also performed on deficiency chromosomes mapping in the 68A region that were heterozygous with a wild-type third chromosome. These results show that *JIL-1* is not removed in *Df(3L)lxd8* (*lxd8*) or *Df(3L)vin3* (*vin3*) but is removed in *Df(3L)vin2* (*vin2*) since hybridization is observed only to the wild-type chromosome but not to the deficiency chromosome. A 5′-*JIL-1* probe hybridizes to *Df(3L)h9* (*h9* 5′) whereas a 3′-*JIL-1* probe does not (*h9* 3′). Arrows depict *JIL-1* hybridization signal. (B) Physical map (modified from CROSBY and MEYEROWITZ 1986) showing regions removed by different deficiency chromosomes (depicted by solid bars) relative to the polytene chromosome in region 67F–69A. Distal is to the left and proximal is to the right. Whether or not the *JIL-1* probe was able to hybridize to these deficiency chromosomes is indicated by a "+" or a "−" to the left of the bar. "+/−" for *Df(3L)h9* (*h9*) indicates that only 5′-*JIL-1* but not 3′-*JIL-1* sequences can hybridize to this deficiency chromosome. The *JIL-1* locus maps within the region depicted by vertical dashed lines, defined by *in situ* hybridization as being proximal to *Df(3L)lxd8* (*lxd8*) and distal to *Df(3L)h76* (*h76*). In addition, the location of the following deficiencies is depicted: *Df(3L)vin4* (*vin4*), *Df(3L)vin5* (*vin5*), and *Df(3L)lxd6* (*lxd6*). (C) Physical and genetic map showing position of the *JIL-1* locus relative to the physical regions removed by deficiency chromosomes *Df(3L)lxd8*, *Df(3L)h9*, and *Df(3L)h76*. Genetic complementation groups previously mapped to this region are uncovered by the indicated deficiency chromosomes (lines below solid bar). The "*D*," "*J*," and "*E*" complementation groups of CAMPBELL *et al.* (1986) correspond to *l(3)68Ad*, *l(3)68Ae*, and *l(3)68Ag* as shown. *l(3)517* (SHEARN *et al.* 1971) corresponds to *l(3)68Ag*. The map position for these alleles is supported by failure to complement with the indicated overlapping deficiency chromosome(s) but ability to complement with *JIL-1* mutant alleles.

genin-labeled *JIL-1* cDNA to Oregon-R polytene chromosomes we mapped the *JIL-1* locus to the 68A region of the third chromosome of Drosophila (Figure 1A). To further refine its localization, cDNA probes were generated containing the 5′ end, the middle, or the 3′ end of the *JIL-1* cDNA sequence. These were hybridized to salivary gland chromosomes from eight different deficiency lines containing deletion-removing portions of the 68A–C region. As shown in Figure 1, A and B, *JIL-1* probes hybridized to chromosomes containing *Df(3L)vin3*, *Df(3L)vin4*, *Df(3L)lxd8*, and *Df(3L)h76*, but not to chromosomes containing *Df(3L)vin2*, *Df(3L)vin5*, and *Df(3L)lxd6*. These results indicate that the *JIL-1* locus is in region 68A4–5 between the proximal and distal deletion breakpoints of *Df(3L)lxd8* and *Df(3L)h76*, respectively. One of the deletions, *Df(3L)h9*, removes the 3′ but not the 5′ end of the *JIL-1* gene (Figure 1A), thus localizing the proximal breakpoint of this deletion within the *JIL-1* locus (Figure 1C). By PCR and DNA sequencing we determined that *Df(3L)h9* removes *JIL-1* sequences beyond nucleotide 3398 of the JIL-1 cDNA sequence, completely removes the two distal genes *CG7839* and *CG6302*, and removes sequences encoding *CG7858* sequences beyond nucleotide 1012 of the three predicted transcripts now designated as *CG33048-RA*, *CG33048-RB*, and *CG33048-RC*. These putative transcript alterations are the consequence of genomic sequence deletion-removing nucleotides 183,457–193,722 of genomic scaffold AE003546 (GI:23093654; Berkeley *Drosophila* Genome Project release 3.0; Figure 2A). The juxtaposition of *Df(3L)h9* deficiency breakpoints results in an immediate in-frame stop codon in the *JIL-1* coding sequence in kinase domain II (KDII) after amino acid 795, thus encoding a truncated JIL-1 protein consisting of the NH_2-terminal domain (NTD), KDI, and most of KDII with no novel sequences present (Figure 2B).

The 68A–C region has been the target of several previous mutagenesis studies (CAMPBELL *et al.* 1986; CROSBY and MEYEROWITZ 1986; STAVELEY *et al.* 1991) identifying multiple lethal complementation groups as shown in Figure 1C. To test whether any of these groups might represent additional alleles of *JIL-1*, we used a full-length JIL-1-expressing transgenic line previously shown capable of rescuing *JIL-1* null and hypomorphic alleles (WANG *et al.* 2001) for rescue experiments. We found that none of the lethal complementation groups mapping in the 68A4–5 region (Figure 1C) could be rescued by this approach. That these alleles do not correspond to *JIL-1* mutations was further confirmed by their ability to complement *JIL-1* null and hypomorphic alleles and

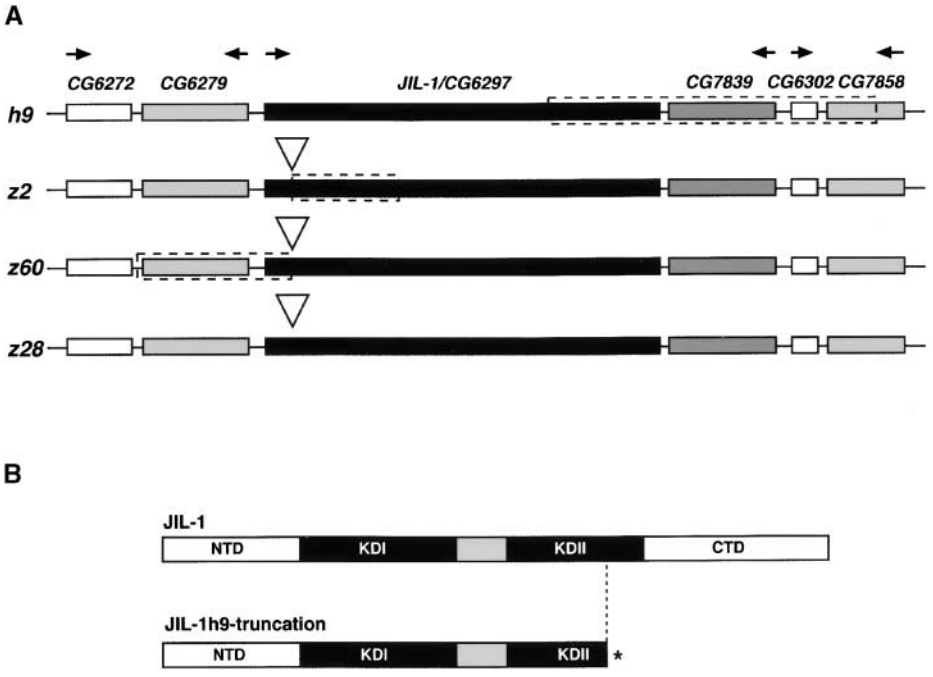

FIGURE 2.—Characterization and mapping of *JIL-1* alleles. (A) Diagrams of lesions in *JIL-1* alleles. Known and predicted genes in the 68A4-5 region are depicted as boxes. The Celera Genomics annotation numbers and direction of transcription are shown at the top. Shaded boxes indicate the region deleted in *Df(3L)h9* (*h9*) and those sequences removed in the imprecise excision lines $JIL\text{-}1^{z2}$ (*z2*) and $JIL\text{-}1^{z60}$ (*z60*) generated from the EP element insertion line $JIL\text{-}1^{EP(3)3657}$ (WANG *et al.* 2001). In *Df(3L)h9*, three genes distal to *JIL-1* (*CG7839*, *CG6302*, and *CG7858*) are also fully or partially deleted as indicated, whereas for $JIL\text{-}1^{z60}$ the proximal gene (*CG6279*) has been completely removed. The $JIL\text{-}1^{z2}$ deletion removes the start codon of the *JIL-1* open reading frame, giving rise to a true null, whereas the $JIL\text{-}1^{z60}$ deletion removes upstream sequences but leaves the EP promoter intact. The $JIL\text{-}1^{z28}$ deletion removes only EP element sequences but leaves the EP promoter region intact. The triangle depicts the insertion site of the EP element in $JIL\text{-}1^{EP(3)3657}$. (B) Schematic of protein products generated by the *JIL-1* alleles. The $JIL\text{-}1^{EP(3)3657}$, $JIL\text{-}1^{z60}$, and $JIL\text{-}1^{z28}$ alleles give rise to a full-length JIL-1 protein composed of an NTD, COOH-terminal domain (CTD), and two kinase domains (KDI and KDII), albeit at lower levels than those of wild type. The $JIL\text{-}1^{h9}$ allele gives rise to a truncated protein (JIL-1h9-truncation) composed of NTD, KDI, and most of KDII, but completely lacking the CTD. Because of the presence of an in-frame stop codon generated precisely at the deficiency breakpoint, there are no novel sequences in the truncated JIL-1 product.

by their localization to chromosomal regions removed in either *Df(3L)lxd8* or *Df(3L)h76* (Figure 1C). Moreover, chromosomes with *Df(3L)lxd8* or *Df(3L)h76* complement the null allele $JIL\text{-}1^{z2}$, indicating that these deficiencies do not remove essential regulatory regions of *JIL-1*, which would not have been detected in our cDNA hybridization analysis. Two of the lethal complementation groups [*l(3)68Ad* and *l(3)01239*] were also removed in *Df(3L)h9*, thus causing homozygous lethality for this deficiency. However, the truncated *JIL-1* allele encoded by this chromosome (Figures 1C and 2B) was able to partially rescue lethal null *JIL-1* animals to adulthood when heterozygous, although surviving adults were sterile (Table 1), suggesting that the truncated JIL-1 protein has a partial function.

Genomic characterization of *JIL-1* null and hypomorphic alleles: By screening GenBank with the *JIL-1* cDNA sequence, we previously identified a *P*-element insertion line ($JIL\text{-}1^{EP(3)3657}$) in which the inducible overexpression EP element (RØRTH *et al.* 1998) had inserted into *JIL-1*'s first exon ~700 bp upstream of the putative start codon, resulting in a decrease in JIL-1 protein expression levels to only ~10% that of wild type (WANG *et al.* 2001). This low-level expression was sufficient to permit ~80% (as compared to wild type) of homozygous animals from heterozygous ($JIL\text{-}1^{EP(3)3657}$/+) parents to eclose, although subsequent generations showed further decreased viability, probably due to decreased levels of maternal product. In our previous study, we used imprecise excision from $JIL\text{-}1^{EP(3)3657}$ to generate a hypomorphic series of *JIL-1* alleles (WANG *et al.* 2001). To further molecularly characterize the nature of these excisions, we performed PCR mapping and DNA sequence analysis. Figure 2A depicts the *JIL-1* genomic region and those sequences that are missing for each of the *JIL-1* alleles (shaded boxes). The $JIL\text{-}1^{z2}$ null allele removes nucleotide 204,172 to sequences within the region between nucleotides 198,609 and 197,546 in the genomic scaffold AE003546, thus removing the *JIL-1* starting ATG codon along with sequences extending into the second intron, as well as deleting the EP element's promoter sequences. We could not assign the precise nucleotide of the breakpoints due to limits of resolution in our PCR mapping approach. The severe hypomorph $JIL\text{-}1^{z60}$ removes the entire *JIL-1* promoter region in addition to the 5′ untranslated region but retains the EP promoter element, thus accounting for the low level of JIL-1 protein observed. However, proximal genomic sequences upstream of *JIL-1*, extending to a region localized between nucleotides 207,742 and 269,371 of the AE003546 genomic scaffold, are also removed, resulting in the loss of the entire *CG6279* coding sequence as well (Figure 2A). Another and previously unreported imprecise excision line from the excision performed by WANG *et al.* (2001), $JIL\text{-}1^{z28}$, does not remove the *JIL-1* sequence but is an imprecise excision of the *EP(3)3657* element that leaves ~3.6 kb of

TABLE 1

Viability of *JIL-1* mutants

	Male genotype					
Female genotype	*z2/TM3*	*h9/TM3*	*z60/TM3*	*EP3/TM3*	*z28/TM3*	*Scim/TM3*
z2/TM3	0.00 (0/538)	0.13 (59/451)	0.18 (118/647)	0.44 (208/477)	0.95 (537/568)	0.88 (170/193)
h9/TM3	0.44 (170/386)	0.00 (0/239)	ND	0.80 (362/454)	0.81 (229/283)	0.86 (211/246)
z60/TM3	0.40 (164/456)	0.33 (80/240)	0.17 (127/761)	0.59 (399/674)	0.85 (469/551)	1.00 (249/249)
EP3/TM3	0.54 (182/340)	0.76 (130/183)	0.60 (307/514)	0.79 (449/570)	0.79 (420/534)	1.06 (164/154)
z28/TM3	0.89 (415/465)	0.80 (176/221)	0.88 (319/361)	0.86 (438/512)	0.66 (428/652)	0.88 (229/261)
Scim/TM3	0.86 (449/525)	0.82 (164/199)	ND	0.81 (321/396)	0.82 (306/374)	1.01 (135/134)

Viability is calculated as the number of observed non-*Tb Hu e* flies/number of the expected Mendelian class of non-*Tb Hu e JIL-1/JIL-1* mutant flies (predicted to be one-half of the number of observed *Tb Hu e* flies). ND, not determined.

the original EP element. Both $JIL\text{-}1^{z60}$ and $JIL\text{-}1^{z28}$ retain the EP GAL4-binding sites and minimal heat-shock promoter.

Reduction in the level of JIL-1 protein is correlated with reduced viability at multiple stages of development: To compare the relative phenotypic effects of the *JIL-1* alleles described above as well as the previously described $JIL\text{-}1^{Scim}$ allele (Dobie *et al.* 2001), each was examined in a series of diallelic crosses. Individuals with different homozygous or heterozygous *JIL-1* genotypes were generated by crossing males and females containing different *JIL-1* alleles and the strength of each mutant genotype was measured by its effect on survival to adulthood (defined here as "viability"). The loss of other genes in the $JIL\text{-}1^{h9}/JIL\text{-}1^{h9}$ and $JIL\text{-}1^{z60}/JIL\text{-}1^{z60}$ homozygotes (see Figure 2A) precludes a direct comparison of the *JIL-1* effects of these alleles on viability in homozygotes. However, viability of each *JIL-1* allele can be assayed when heterozygous with the null $JIL\text{-}1^{z2}$ allele. This analysis revealed a general trend from least to most viable of $JIL\text{-}1^{z2} < JIL\text{-}1^{h9} < JIL\text{-}1^{z60} < JIL\text{-}1^{EP(3)3657} < JIL\text{-}1^{z28} \sim JIL\text{-}1^{Scim}$ (Table 1). This order of severity is preserved in most of the possible allelic combinations with the exception of the $JIL\text{-}1^{z28}/JIL\text{-}1^{z28}$ homozygote, which is less viable than expected, given its mild decrease in viability in all other combinations. This result may indicate an as-yet-undefined second site aberration on this chromosome. In the cases of $JIL\text{-}1^{z28}$ and $JIL\text{-}1^{Scim}$, JIL-1 levels appear to be sufficient to mask differences between levels of the other alleles as measured by the rate of adult eclosion.

To determine whether the degree of viability in the allelic series corresponded to levels of JIL-1 protein produced in different mutant backgrounds, protein extracts from homozygous *JIL-1* mutant third instar larvae were analyzed by Western blotting using an antibody probe directed against the JIL-1 COOH-terminal domain (Jin *et al.* 1999). Figure 3 shows the results of such an experiment. JIL-1 protein levels as compared to wild type (defined as 100%) were 0% for $JIL\text{-}1^{z2}$, 0.3% for $JIL\text{-}1^{z60}$, 5% for $JIL\text{-}1^{EP(3)3657}$, 45% for $JIL\text{-}1^{z28}$, and 58% for $JIL\text{-}1^{Scim}$. This comparison of protein levels allows the *JIL-1* alleles to be arranged in an allelic series, $JIL\text{-}1^{z2} < JIL\text{-}1^{z60} < JIL\text{-}1^{EP(3)3657} < JIL\text{-}1^{z28} < JIL\text{-}1^{Scim}$, which is identical to that obtained from examining viability. Thus a direct correlation was observed between the level of JIL-1 protein and the severity of mutant effect on adult viability. The $JIL\text{-}1^{h9}$ allele was not included in the Western blot analysis since the loss of JIL-1 COOH-terminal sequences precludes its detection using this antibody. However, by Northern blotting we found that the $JIL\text{-}1^{h9}$ allele produces a shorter *JIL-1* transcript present at levels equivalent to full-length *JIL-1* transcript from the *TM3*

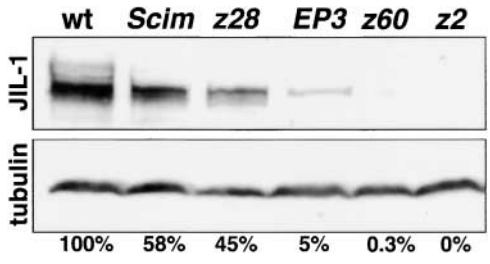

Figure 3.—JIL-1 protein expression in *JIL-1* hypomorphic and null alleles. Immunoblots were performed on extracts from homozygous $JIL\text{-}1^{Scim}$ (*Scim*), $JIL\text{-}1^{z28}$ (*z28*), $JIL\text{-}1^{EP(3)3657}$ (*EP3*), $JIL\text{-}1^{z60}$ (*z60*), and $JIL\text{-}1^{z2}$ (*z2*) larvae and compared to wild type (wt). The immunoblots were labeled with affinity-purified JIL-1 antiserum and with antitubulin antibody. The relative level of JIL-1 expression in the mutant larvae as a percentage of JIL-1 expression in wild type is shown below.

balancer chromosome (data not shown). This—in conjunction with the ability of *JIL-1^{h9}* to partially rescue the null *JIL-1^{z2}* allele to yield *JIL-1^{h9}/JIL-1^{z2}* viable, albeit sterile, adults (see below)—suggests that the truncated protein can provide partial JIL-1 function.

A second trend apparent from the results shown in Table 1 is that the genotype of the female parent has a more significant effect on viability than that of the male parent. When females heterozygous for the null *JIL-1^{z2}* allele are crossed with males containing other alleles, fewer progeny are produced than in the reciprocal crosses. In crosses with the weaker *JIL-1^{z28}* and *JIL-1^{Scim}* alleles, these alleles' levels of JIL-1 protein appear sufficient to mask the maternal effect of *JIL-1^{z2}*. These results suggest that *JIL-1* alleles have a maternal effect. To further test for a *JIL-1* maternal effect, we performed a series of reciprocal crosses. The first was a set of crosses between individuals with *JIL-1^{z2}/JIL-1$^{EP(3)3657}$* and wild-type genotypes, the second was a set of crosses between individuals with *JIL-1^{z2}/JIL-1$^{EP(3)3657}$* and *JIL-1^{z2}/TM3* genotypes, and the third was a cross between *JIL-1^{z2}/TM6* males and females (Table 2). For each cross, three sets of data were obtained. First, embryonic viability was determined by measuring the hatch rate of fertilized eggs. Second, larval viability was determined by collecting newly hatched first instar larvae and measuring their rate of survival to pupariation. Third, adult viability was determined by measuring the frequency of adult eclosion from pupae. The results are shown in Table 2. In cross 1, only 8% of the fertilized eggs laid by the *JIL-1^{z2}/JIL-1$^{EP(3)3657}$* females hatched, compared with 94% of the eggs laid by wild-type females. Even though the offspring are of the same genotypes (50% *JIL-1^{z2}*/+ and 50% *JIL-1$^{EP(3)3657}$*/+), more larvae with wild-type female parents survived to pupation (95 *vs.* 58%). Of the individuals who pupariated, about the same fraction survived to eclosion (94% from *JIL-1^{z2}/JIL-1$^{EP(3)3657}$* females and 96% from wild-type females), indicating that after pupariation this maternal effect is negligible. Thus, these results confirm that *JIL-1* has a maternal effect and suggest that this effect persists throughout the larval period.

These results were further confirmed by the second set of crosses (Table 2, cross 2). In these crosses, as previously observed, the *JIL-1^{z2}/JIL-1$^{EP(3)3657}$* females show a low rate of hatching of fertilized eggs (2%). However, the hatch rate of fertilized eggs laid by the *JIL-1^{z2}/TM3* females (87%) is higher than that of the expected *JIL-1/TM3* Mendelian class (50%), suggesting that many embryos with a *JIL-1^{z2}/JIL-1^{z2}* or *JIL-1^{z2}/JIL-1$^{EP(3)3657}$* genotype can complete embryonic development if provided with normal maternal JIL-1 product. No *JIL-1^{z2}/JIL-1^{z2}* progeny survive to eclosion and the number of surviving *JIL-1^{z2}/JIL-1$^{EP(3)3657}$* adults is about half that of comparable sibling genotypic classes. The reduced rate of survival to pupariation (59%) suggests that some *JIL-1^{z2}/JIL-1^{z2}* and *JIL-1^{z2}/JIL-1$^{EP(3)3657}$* individuals fail to survive the larval period. Therefore, in the third cross (Table 2, cross 3) we made use of a *TM6* balancer chromosome that contains *Sb* and *Tb* alleles. *Sb* is homozygous lethal with an early embryonic lethal period, and no *TM6/TM6* individuals hatch from the egg. The *Tb* allele marks larvae and pupae, allowing us to track the survival of the *JIL-1^{z2}/JIL-1^{z2}* individuals during the larval and pupal periods. The percentage of eggs that did not hatch was 29%, which is close to the percentage expected due to lethality of the homozygous *TM6/TM6* individuals (25%). This suggests that most *JIL-1^{z2}/JIL-1^{z2}* embryos produced by a heterozygous mother complete embryonic development. Since all or most of the *JIL-1^{z2}/JIL-1^{z2}* embryos hatch, one-third of the collected larvae would be expected to be of the *JIL-1^{z2}/JIL-1^{z2}* genotype. Only 251 *JIL-1^{z2}/JIL-1^{z2} (Tb^{+})* larvae pupariated compared with 1325 *JIL-1^{z2}/TM6 Tb* larvae. This suggests that a significant fraction of the *JIL-1^{z2}/JIL-1^{z2}* individuals die during the larval period. None of the *JIL-1^{z2}/JIL-1^{z2}* individuals that pupariate survive to adult eclosion. In contrast, almost all of the *JIL-1^{z2}/TM6* individuals (96%) who pupariate survive to adult eclosion.

To determine whether the observed maternal effects correlated with the *JIL-1* allelic series (Table 1), we performed crosses testing for maternal effects using different *JIL-1* alleles (Table 3). In these crosses females with *JIL-1^{z2}/JIL-1^{h9}*, *JIL-1^{z2}/JIL-1$^{EP(3)3657}$*, *JIL-1^{z2}/JIL-1^{z28}*, or *JIL-1^{z2}/JIL-1^{Scim}* genotypes were mated to males with a +/+ genotype. For each cross, the rates of hatching, pupariation, and adult eclosion were determined (Table 3). Despite the contribution of a wild-type *JIL-1* allele from the father to the fertilized embryo, the reduction in maternal JIL-1 due to the mother's genotype resulted in decreased hatch rates, ranging from 0% for *JIL-1^{z2}/JIL-1^{h9}* females to 8% for *JIL-1^{z2}/JIL-1$^{EP(3)3657}$* females to 41% for *JIL-1^{z2}/JIL-1^{z28}* females to 60% for *JIL-1^{z2}/JIL-1^{Scim}* females. This decrease in maternal effect for *JIL-1* hypomorphic alleles correlates well with the allelic series of *JIL-1^{h9}* < *JIL-1$^{EP(3)3657}$* < *JIL-1^{z28}* ~*JIL-1^{Scim}* determined in Table 1. The *JIL-1^{z2}* allele is not included in this assay since *JIL-1^{z2}/JIL-1^{z2}* adult females cannot be generated for this cross due to *JIL-1^{z2}* being homozygous lethal. The effect on egg production due to loss of maternal JIL-1 in the *JIL-1^{z2}/JIL-1^{h9}* females was remarkable. For all of the other *JIL-1* alleles, a total of 25 females were used in each cross and each female laid between 12 and 20 eggs per day. For the *JIL-1^{z2}/JIL-1^{h9}* cross a total of 125 females were used, and even so, very few eggs were laid and none hatched.

The above crosses illustrate the requirement for JIL-1 during larval development as evidenced by decreased pupariation rates of *JIL-1* heterozygous mutant larvae. The percentage of the collected larvae that pupariated was 58, 71, and 80% for *JIL-1$^{EP(3)3657}$/JIL-1^{z2}*, *JIL-1^{z28}/JIL-1^{z2}*, and *JIL-1^{Scim}/JIL-1^{z2}*, respectively. Thus, the decrease in pupariation observed with the hypomorphic alleles correlated with their level of reduction of JIL-1 protein (Figure 3), namely *JIL-1$^{EP(3)3657}$* < *JIL-1^{z28}* < *JIL-1^{Scim}*. To

TABLE 2

Reciprocal crosses of male and female *JIL-1* mutant alleles

Female genotype	Male genotype	Hatch rate (larvae/total eggs)	Pupariation rate (pupae/total larvae)	Eclosion rate (adult/total pupae)			
			Cross 1				
z2/EP3	+/+	0.08 (170/2195)	0.58 (77/133)	0.94 (73/77)			
+/+	*z2/EP3*	0.94 (2343/2484)	0.95 (1492/1559)	0.96 (1433/1492)			
				Genotype and no. of eclosed flies			
Female genotype	Male genotype	Hatch rate (larvae/total eggs)	Pupariation rate (pupae/total larvae)	*z2/z2*	*z2/EP3*	*z2/TM3*	*EP3/TM3*
			Cross 2				
z2/EP3	*z2/TM3*	0.02 (36/2413)	0.76 (19/25)	0	0	0	15
z2/TM3	*z2/EP3*	0.87 (2139/2452)	0.59 (823/1406)	0	154	311	301
			Pupariation rate of F_1 larval genotypes		Eclosion rate of F_1 pupal genotypes		
Female genotype	Male genotype	Hatch rate (larvae/total eggs)	*z2/z2*	*z2/TM6*	*z2/z2*	*z2/TM3*	
			Cross 3				
z2/TM6	*z2/TM6*	0.71 (2242/3170)	0.35[a] (251/722)	0.92[b] (1325/1443)	0 (0/251)	0.96 (1268/1325)	

[a] Number of expected pupae is one-third of the total number of larvae examined.
[b] Number of expected pupae is two-thirds of the total number of larvae examined.

TABLE 3

Maternal effect of different *JIL-1* genotypes

Female genotype	Male genotype	Hatch rate (larvae/total eggs)	Pupariation rate (pupae/total larvae)	Eclosion rate (adult/pupae)
z2/h9	+/+	0.00 (0/86)	NA	NA
z2/EP3	+/+	0.08 (170/2195)	0.58 (77/133)	0.95 (73/77)
z2/z28	+/+	0.41 (785/1907)	0.71 (469/665)	0.94 (440/469)
z2/Scim	+/+	0.60 (1274/2119)	0.80 (869/1084)	0.94 (818/869)
+/+	+/+	0.91 (1431/1579)	0.95 (996/1052)	0.98 (975/996)

NA, not applicable.

test whether the genetic requirement for *JIL-1* function at different developmental stages correlated with the presence of JIL-1 protein, we performed a developmental Western blot analysis. Protein extracts from staged embryos, larvae, pupae, and adults were fractionated on SDS-PAGE, transferred to nitrocellulose, and probed with antibody directed against the JIL-1 COOH-terminal domain (Jin *et al.* 1999). Figure 4 shows the results of such an experiment. JIL-1 protein is detected at significant levels throughout development, including appreciable levels of JIL-1 in 0- to 2-hr embryos as would be expected given *JIL-1*'s maternal effect.

JIL-1 is required for normal larval polytene chromosome structure: We have previously shown that severe loss-of-function *JIL-1* mutations result in aberrant larval polytene chromosome structure (Wang *et al.* 2001), but because few or none of these mutant animals survive to adulthood, it is possible that the chromosomal aberrations are an indirect consequence of impending loss of viability. Since *JIL-1^{h9}/JIL-1^{z2}* animals can survive to adulthood, they afforded an opportunity to compare the polytene chromosome morphology of these animals with that of homozygous *JIL-1* null animals (Figure 5). However, since the *JIL-1^{h9}* deficiency also removes sequences from three other genes (Figure 2), we needed to assess whether any chromosomal phenotype was associated with the resulting hemizygosity of these genes. Polytene chromosomes from animals with a *Df(3L)h9/+* genotype were squashed and stained with Hoechst. Both male and female polytene chromosomes exhibited normal morphology with clearly defined Hoechst-stained bands of heterochromatic-like regions interspersed with less intensely stained euchromatic interbands (Figure 5, A and B). This staining pattern was indistinguishable from that of wild type (data not shown). However, when

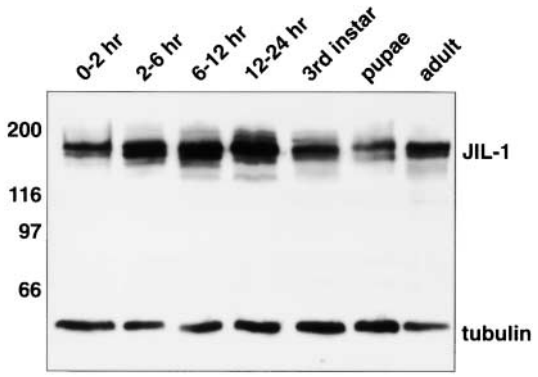

Figure 4.—Developmental Western blot analysis of JIL-1 protein. Protein extracts from selected stages of Drosophila development were fractionated by SDS-PAGE, immunoblotted, and labeled with JIL-1-specific antibody (JIL-1) or with tubulin antibody as a control (tubulin). The JIL-1 protein is present throughout development. The migration of molecular mass markers in kilodaltons is indicated to the left.

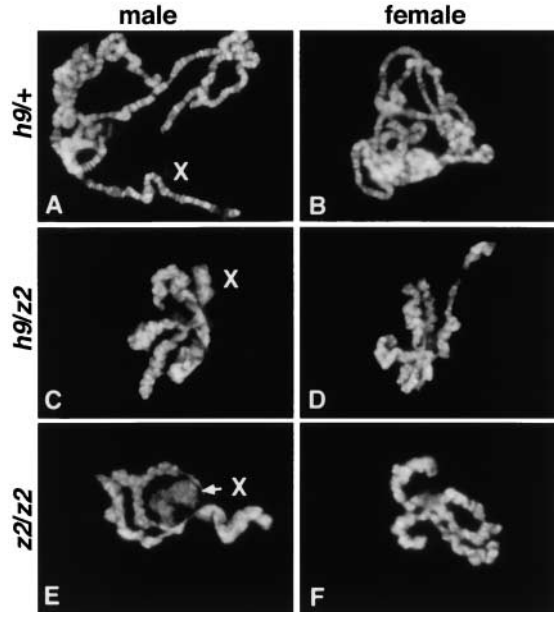

Figure 5.—The *JIL-1^{h9}* allele has a severe effect on the structure and morphology of male and female larval polytene chromosomes. Polytene chromosome preparations from third instar larvae were labeled with Hoechst to visualize the chromatin. The male X chromosome is indicated with an X. Preparations are shown from male and female *JIL-1^{h9}/+* (*h9/+*) heterozygous larvae (A and B), from *JIL-1^{h9}/JIL-1^{z2}* (*h9/z2*) heterozygous larvae (C and D), and from *JIL-1^{z2}/JIL-1^{z2}* (*z2/z2*) homozygous larvae (E and F).

the *Df(3L)h9* chromosome was paired with a chromosome containing the *JIL-1^{z2}* mutant allele, a severe perturbation of chromosome structure was observed (Figure 5, C and D). The autosomes appear highly coiled and compact, and the interband regions, which are normally distinguished by lower levels of Hoechst staining, are lost. In males, the X chromosome is even shorter and in addition exhibits a "puffy" morphology (Figure 5C). This phenotype is highly penetrant and was observed in all animals analyzed ($n > 10$). Although many of these larvae go on to develop into adults, this phenotype is very similar to the homozygous null *JIL-1^{z2}/JIL-1^{z2}* phenotype (Figure 5, E and F), although the "puffing" of the X chromosome in males in the homozygous null *JIL-1* background tends to be more extreme (Figure 5E).

JIL-1 is required for normal oogenesis: Since *JIL-1* shows a strong maternal effect, we expected that mutations in *JIL-1* might also affect the process of oogenesis. For this reason we examined ovaries and egg chambers in *JIL-1^{h9}/JIL-1^{z2}* and *JIL-1$^{EP(3)3657}$/JIL-1$^{EP(3)3657}$* mutant backgrounds. *JIL-1^{h9}/JIL-1^{z2}* animals eclose at a reduced rate but those animals that survive to adulthood are sterile and females produce eggs at a significantly lower level. Even though we used five times more females in the *JIL-1^{h9}/JIL-1^{z2}* crosses to produce eggs to generate the data for Table 3, we obtained <4% of the total number of eggs that we obtained when *JIL-1^{z2}* was in combination with any other *JIL-1* allele. None of the eggs were able to hatch (Table 3). Homozygous *JIL-1$^{EP(3)3657}$/JIL-1$^{EP(3)3657}$* mothers lay eggs at a significantly higher rate than *JIL-1^{h9}/JIL-1^{z2}* mothers but the hatch rate of those eggs is <10% (Wang *et al.* 2001; Zhang *et al.* 2003; this study). To compare the effect of *JIL-1* mutations in egg production, ovaries were dissected from wild-type, *JIL-1$^{EP(3)3657}$/JIL-1$^{EP(3)3657}$*, *JIL-1^{h9}/JIL-1^{z2}*, or *JIL-1^{h9}/+* females. Images of dissected ovaries were obtained on a stereomicroscope using a digital camera and the relative size of each ovary determined in square millimeters. A moderate decrease in size was observed for the *JIL-1$^{EP(3)3657}$/JIL-1$^{EP(3)3657}$* mutant ovaries (average size 0.25 ± 0.10 mm^2, $n = 23$) as compared with wild type (average size 0.40 ± 0.08 mm^2, $n = 19$). The *JIL-1^{h9}/JIL-1^{z2}* mutant ovaries, however, showed a significant ($P < 0.05$, Student's *t*-test) decrease in size, averaging 0.05 ± 0.07 mm^2 ($n = 23$). Ovaries from *JIL-1^{h9}/+* females (average size 0.42 ± 0.08 mm^2, $n = 19$) were indistinguishable from those of wild type ($P > 0.90$, Student's *t*-test), suggesting that the *JIL-1^{h9}/JIL-1^{z2}* phenotype is caused by a defect in the *JIL-1* locus and not by any of the other genes removed by the *Df(3L)h9* deficiency. Examples of the range of phenotypes observed are shown in Figure 6. In most cases, *JIL-1^{h9}/JIL-1^{z2}* ovaries consisted primarily of connective tissue with little or no apparent ovariole development (Figure 6F). However, in a smaller number of cases *JIL-1^{h9}/JIL-1^{z2}* ovary tissue developed to some degree. An example of such an ovary pair is shown in Figure 6E. However, all ovaries examined in these *JIL-1* mutant backgrounds were clearly defective in size and overall morphology.

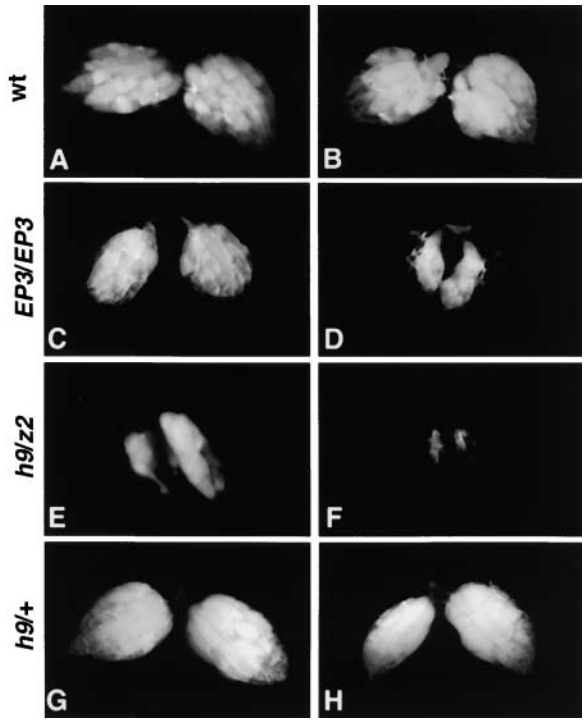

Figure 6.—Effect of *JIL-1* mutations on ovary size. Ovaries dissected from wild-type (wt) and *JIL-1* mutant females. Mutant ovaries from *JIL-1$^{EP(3)3657}$/JIL-1$^{(EP(3)3657}$* (*EP3/EP3*) homozygous females were consistently smaller in size (C and D) than those from wild-type flies (A and B). Ovaries from *JIL-1^{h9}/JIL-1^{z2}* heterozygous flies (*h9/z2*) show only minimal development (E) and in many cases fail to develop at all (F). Animals that are heterozygous for the *Df(3L)h9* chromosome with a wild-type chromosome (*h9/+*) are indistinguishable from wild type (G and H).

Consequently, the low level of egg laying from *JIL-1^{h9}/JIL-1^{z2}* females likely reflects how few of these animals appear to have differentiated germline tissue. However, from those ovaries that do show some degree of tissue development, fixation and Hoechst staining reveal a number of severe anatomical defects as compared to wild type. In normal egg-chamber development, 15 of the 16 interconnected germline cells undergo multiple rounds of DNA replication in the absence of division (reviewed in Mahowald and Kambysellis 1980), giving rise to large, polyploid nurse cell nuclei (Figure 7A). A layer of somatically derived follicle cells surround the developing egg chamber, and the diploid germline-derived oocyte cell gradually enlarges during maturation with its nucleus localizing posteriorly (reviewed in Spradling *et al.* 1997). In the *JIL-1^{h9}/JIL-1^{z2}* females, we observed a range of phenotypes with the most common defect consisting of egg chambers with a reduction in numbers of nurse cells and no apparent oocyte nucleus (Figure 7D). In other cases cell nuclei appear to either

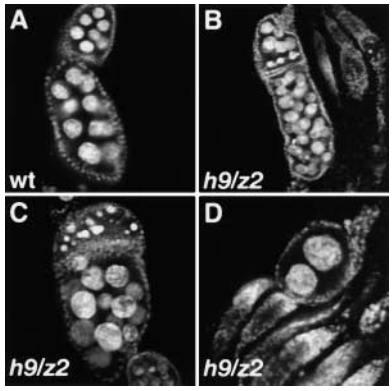

FIGURE 7.—Egg-chamber development in *JIL-1^{h9}/JIL-1^{z2}* ovaries. Ovaries from either wild-type or mutant *JIL-1^{h9}/JIL-1^{z2}* females were dissected, fixed, and stained with Hoechst to analyze egg-chamber development within individual ovarioles. (A) Wild-type egg chambers (wt) show a regular array of large polyploid nurse cell nuclei developing within each follicle. *JIL-1^{h9}/JIL-1^{z2}* (*h9/z2*) mutant egg chambers show a range of defects, including too many nurse cell nuclei encapsulated within an egg chamber (B), fragmentation of nuclei and/or smaller nuclei (C), and too few nurse cell nuclei encapsulated within an individual egg chamber (D). Note the occurrence of apparently "empty" ovarioles and egg chambers in the different classes of phenotypes (B and D).

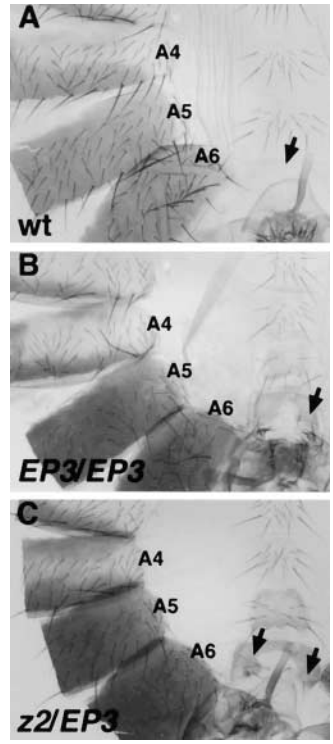

FIGURE 8.—*JIL-1* mutants exhibit posterior-to-anterior homeotic transformations. Abdominal cuticle preparations from adult male flies. Dorsal is to the left and anterior is to the top. (A) In wild-type (wt) male flies the unpigmented ventral A6 sternite is broad and contains no bristles (arrow) whereas more anterior sternites are covered by large bristles. (B) In *JIL-1$^{EP(3)3657}$/JIL-1$^{EP(3)3657}$* (*EP3/EP3*) mutant animals, bristles are found on the A6 sternite (arrow), indicating a transformation toward A5. (C) In *JIL-1^{z2}/JIL-1$^{EP(3)3657}$* (*z2/EP3*) mutant animals, the transformation of A6 toward A5 is indicated by ventral sternite bristles (arrows).

fragment or fail to undergo DNA amplification properly, resulting in obvious defects in egg-chamber development (Figure 7C). In a smaller number of cases, increased numbers of nurse cells were observed, which may reflect fused egg chambers (Figure 7B). In all such phenotypic classes, other ovarioles within the same ovary often appeared empty with no egg chambers formed (Figure 7, B and D). This observation is consistent with the consistently smaller-sized ovaries found in *JIL-1^{h9}/JIL-1^{z2}* females (Figure 6).

***JIL-1* mutants exhibit posterior-to-anterior homeotic transformations:** In Drosophila, segment identity is determined by the proper expression of homeotic genes in each segment. Segment identity is initially established at early embryonic stages by gap and pair-rule genes (SIMON *et al.* 1990; QIAN *et al.* 1991; MULLER and BIENZ 1992; SHIMELL *et al.* 1994). However, their expression is only transient and the maintenance of proper expression of homeotic genes has been attributed to trithorax group (trxG) and polycomb group (PcG) proteins during the remaining life stages. trxG proteins have been shown to be involved in the maintenance of transcriptionally active chromatin while PcG proteins help to maintain an inactive chromatin structure (reviewed in ORLANDO and PARO 1995; SIMON 1995). Since JIL-1 is also involved in control of chromatin structure (WANG *et al.* 2001), we examined whether alleles of *JIL-1* also could give rise to homeotic transformation phenotypes. As shown in Figure 8 in wild-type males, the unpigmented ventral cuticular plate (sternite) of the abdominal sixth segment (A6) is not covered by large bristles, while sternites of more anterior segments are. However, in 88% (n = 58) of *JIL-1$^{EP(3)3657}$* homozygous males the A6 sternite is covered by one or more large bristles, suggesting a transformation of A6 to the more anterior A5 segment (Figure 8B). Of *JIL-1^{z2}/JIL-1$^{EP(3)3657}$* heterozygous males, 93% (n = 40) displayed the same phenotype (Figure 8C). Furthermore, we observed frequent ectopic trichomes on the A6 tergite in *JIL-1* mutant females but not in wild-type females (data not shown). These phenotypes are comparable to those characteristic of *trxG* mutations (INGHAM and WHITTLE 1980; SHEARN 1989) and suggest that *JIL-1* might play a similar role as other previously described trxG proteins in maintaining an open chromatin structure at the *BX-C* locus.

To test whether JIL-1 may have regulatory functions in *BX-C* expression analogous to those previously identified for *trxG* genes (reviewed in ORLANDO and PARO 1995; SIMON 1995), we probed for genetic interactions between *JIL-1* and the known *trxG* genes *brahma* and *trithorax*. The Drosophila *brahma* gene encodes an ATPase that is a catalytic component of a complex similar to the yeast SWI/SNF chromatin remodeling complex

TABLE 4

Genetic interaction between *JIL-1^{Z2}* and *brm^{2} trx^{E2}* alleles

	Male genotype		
Female genotype	+	*JIL-1^{z2}*	*brm^{2} trx^{E2}*
+	0.00[a] (0/200)	0.02 (4/181)	0.17 (17/98)
JIL-1^{z2}	0.02 (5/182)	NA	0.65 (89/137)
brm^{2} trx^{E2}	0.09 (10/110)	0.75 (54/72)	NA

NA, not applicable.

[a] Fraction of male flies exhibiting an A6-to-A5 transformation phenotype.

(Tamkun *et al.* 1992; Papoulas *et al.* 1998). TRITHORAX is a SET domain-containing protein that has been recently found to interact with the catalytic subunit of the serine/threonine protein phosphatase PP1c (Rudenko *et al.* 2003). Since JIL-1 regulates histone H3 phosphorylation in Drosophila and likely has other substrates, it was of interest to test whether *JIL-1*, *brahma*, and *trithorax* have synergistic effects in determining segment identity. To explore this possibility, *JIL-1^{z2}* mutants and *brahma^{2}* (*brm^{2}*) and *trithorax^{E2}* (*trx^{E2}*) double mutants were crossed with a standard *y,w* strain and a wild-type third chromosome, respectively, to serve as controls. As shown in Table 4, in *JIL-1* heterozygotes only 2% of the animals exhibited an A6-to-A5 transformation regardless of whether the *JIL-1^{Z2}* allele had been introduced by the male or the female. This suggests that there is no maternal effect of *JIL-1* on the transformation phenotype. Similarly, *brm^{2}* and *trx^{E2}* double heterozygotes exhibited only moderate ratios (9 and 17% when introduced by the female or male, respectively) of the same A6-to-A5 transformation in reciprocal crosses. In contrast, triple male heterozygotes carrying *JIL-1^{z2}*, *brm^{2}*, and *trx^{E2}* alleles showed a much higher percentage of transformation with 65% exhibiting the transformation phenotype when *JIL-1^{z2}* was contributed by the female and *brm^{2} trx^{E2}* was contributed by the male and a 75% transformation rate in the reciprocal cross. This observed frequency was significantly higher ($P < 0.005$, χ^2 test) than would be expected for a simple additive effect contributed by the mutant alleles from each parent. Thus, this synergistic genetic interaction between *JIL-1^{z2}*, *brm^{2}*, and *trx^{E2}* suggests that JIL-1 participates with other trxG members in the regulation of gene expression at the *BX-C* locus and raises the possibility that similar interactions may also occur on other target genes.

DISCUSSION

In this study we have undertaken a genetic approach to characterize the effect of mutations in the chromosomal kinase JIL-1 on development in Drosophila. We show that the mutations form an allelic series and that viability is directly correlated with JIL-1 protein levels. Furthermore, we provide evidence that JIL-1 function is required at all stages of development, including oogenesis and during embryonic, larval, and pupal stages. However, relatively low levels (5–10%) of JIL-1 protein are sufficient to sustain development into adults and *JIL-1$^{EP(3)3657}$* flies can be maintained as a homozygous stock for at least a few generations (Wang *et al.* 2001). *JIL-1* has a strong maternal effect and some *JIL-1* null offspring produced by heterozygous females can survive on maternally produced JIL-1 until pupariation although they are unable to eclose. In contrast, we detected only a minor effect on embryonic hatch rates by paternally contributed JIL-1.

Using *in situ* hybridization we mapped the *JIL-1* locus to the 68A4–5 region of the larval polytene chromosome. By combining *in situ* hybridization and genetic complementation analysis, we further determined that the *JIL-1* locus lies between the distal breakpoint of *Df(3L)h76* and the proximal breakpoint of *Df(3L)lxd8* with neither deficiency removing essential elements of the *JIL-1* locus. The proximal breakpoint of *Df(3L)h9*, however, falls within *JIL-1* coding sequence and the deficiency removes JIL-1 COOH-terminal sequences as well as all or part of the coding sequences from three distal genes. In agreement with our deficiency mapping results, we found that the *JIL-1* locus did not correspond to previously identified lethal complementation groups that map to the 68A region and are uncovered by *Df(3L)lxd8* or *Df(3L)h76* (Campbell *et al.* 1986; Crosby and Meyerowitz 1986; Staveley *et al.* 1991). Our data confirm the results obtained in mapping studies for another gene in the region, *Su(UR)* (Makunin *et al.* 2002), with the exception that we find that the breakpoints of *Df(3L)h76* and *Df(3L)lxd8* fall proximal and distal to the *JIL-1* locus, respectively, instead of within the *JIL-1* locus.

We molecularly characterized the lesions associated with the various *JIL-1* alleles used in this study, which were mostly generated from imprecise *P*-element excisions (Wang *et al.* 2001). In most cases, these alleles are hypomorphic or null, resulting in a reduction or loss of wild-type JIL-1 protein. In one case, however, the chromosomal aberration associated with *Df(3L)h9* results in the deletion of JIL-1 COOH-terminal sequences, thus encoding a truncated protein that lacks the COOH-terminal domain and conserved subdomains IX–XI of the second kinase domain (Figure 2). Since these subdomains are implicated in stabilizing the kinase's large lobe and catalytic loop (reviewed in Hardie and Hanks 1996), this truncation would be expected to cause loss of kinase activity in KDII. In the related tandem kinase p90 RSK (Johansen *et al.* 1999), the second kinase domain has been shown to be one of the kinases that activate the amino-terminal kinase domain (Dalby *et al.* 1998; Frodin and Gammeltoft 1999). Thus, regula-

tion of JIL-1 kinase activity may be compromised in the *JIL-1^{h9}* truncation. In addition, the *Df(3L)h9* deficiency removes three additional genes. However, the fact that *JIL-1^{h9}*/+ heterozygotes are indistinguishable from wild type suggests that the observed phenotypes are caused by the truncation of JIL-1. Interestingly, this truncated product exhibits partial function. When the *JIL-1^{h9}* allele is heterozygous with the null *JIL-1^{z2}* allele, the eclosion rate is 44% when *JIL-1^{h9}* is provided by the mother but only 13% when provided by the father. This shows that *JIL-1^{h9}* exerts a positive effect on maternal rescue of viability. However, it is noteworthy that even though viability is at least partially restored, the abnormal polytene chromosome phenotype characteristic of *JIL-1^{z2}*/*JIL-1^{z2}* animals is still observed. These results suggest that the COOH-terminal domain and/or the second kinase domain of JIL-1 plays an essential role in establishing or maintaining normal chromatin structure. It is interesting that these animals are able to survive to adulthood despite the significant chromosomal defects observed. The fact that these animals are sterile and exhibit gross ovarian defects and chromosomal abnormalities in the developing oocytes suggests that this region of JIL-1 is essential not only for chromatin structure but also for viability at early stages. The reason that *JIL-1^{h9}*/*JIL-1^{z2}* animals survive past critical earlier imprinting stages when chromatin domains and expression patterns are being specified is likely to be *JIL-1*'s strong maternal effect. Mothers heterozygous for wild-type *JIL-1* are able to provide enough maternal product to allow most of their homozygous *JIL-1^{z2}*/*JIL-1^{z2}* offspring to develop to larval stages and a smaller percentage even to pupate. This "maternal rescue" presumably allows early development of *JIL-1^{h9}*/*JIL-1^{z2}* animals as well.

The importance of the JIL-1 COOH-terminal region is emphasized by the sterility of the *JIL-1^{h9}*/*JIL-1^{z2}* heterozygotes and we show that the size of ovaries as well as oogenesis is strongly affected by this mutation. Oogenesis is a coordinated and complex developmental process involving signals exchanged between nurse and follicle cells (Spradling *et al.* 1997). We found that *JIL-1^{h9}*/*JIL-1^{z2}* females are defective in oogenesis whereas female *Df(3L)h9*/+ heterozygotes are phenotypically wild type. Many mutant egg chambers in *JIL-1^{h9}*/*JIL-1^{z2}* females have aberrant nurse cell numbers. In most of these mutant egg chambers there are fewer nurse cells, but less frequently many more than the normal number of 15 nurse cells can been found in one egg chamber. Similar phenotypes have been previously described in a study identifying mutants in oogenesis that could be categorized into various classes, including reduced nurse cell number and supernumerary nurse cell number (Bellotto *et al.* 2002). Other genes that are known to cause abnormal numbers of nurse cells include *shut down* (*shu*), *stand still* (*stil*), and *stall* (*stl*) (Schüpbach and Wieschaus 1991). These findings suggest that JIL-1 may play a role in the normal progression of early oogenesis and be involved in regulating some of these genes either directly by participating in signal transduction pathways essential for oocyte differentiation or indirectly by affecting chromatin structure and gene expression.

In a similar way, JIL-1 may be involved in the development of segment identity since *JIL-1* mutations can give rise to transformation phenotypes resembling those of alleles of the trithorax-group genes. The appropriate expression of homeotic genes requires coordination of trxG and PcG proteins that form multi-component complexes at regulatory regions of homeotic loci (Shearn 1989; Paro 1990; Pirrotta and Rastelli 1994; Simon 1995). Recent studies have shown that trxG and PcG complexes contain proteins that, similar to JIL-1, are involved in histone covalent modifications or chromatin remodeling (Dingwall *et al.* 1995; Beisel *et al.* 2002; Czermin *et al.* 2002; Muller *et al.* 2002). The *Abdominal-B* (*Abd-B*) gene is one of the three homeotic genes in the *Bithorax-Complex* and controls development of abdominal segments. Mutations in *trxG* genes affecting *Abd-B* expression display posterior-to-anterior segment transformation due to transition of an active chromatin conformation to an inactive one (reviewed in Orlando and Paro 1995). In *JIL-1* mutants, the cells in the A6 abdominal epidermis take the cell fate of the more anterior A5 segment. That *JIL-1* mutants can give rise to phenotypes analogous to those of *trxG* genes and that *JIL-1* acts synergistically with *trxG* genes suggest that JIL-1 may also participate in maintaining an active chromatin structure at these loci.

In addition, JIL-1 recently was found to interact with the developmentally regulated LOLA isoform zf5 (Zhang *et al.* 2003). The *lola* locus is complex and codes for at least 15 different isoforms containing different tandem zinc-finger domains in conjunction with a common BTB dimerization domain (Giniger *et al.* 1994; Zhang *et al.* 2003). Although the physiological role of LOLA zf5 has not been determined, the *lola* locus has been implicated in transcriptional regulation (Giniger *et al.* 1994; Cavarec *et al.* 1997; Crowner *et al.* 2002). An attractive model that has recently been proposed (Ishii and Laemmli 2003) postulates that some transcription factors can regulate gene expression levels by influencing chromatin architecture by serving as boundary elements or desilencing elements. By assembling complexes that can promote silencing or desilencing activities, the expression potential of a chromosomal region can be regulated. By interacting with LOLA isoforms JIL-1 may be involved in such modulation of gene activity.

In summary, our findings suggest that JIL-1 activity is necessary for the normal progression of several developmental processes at different developmental stages. We propose that JIL-1 can exert such pleiotrophic effects either by directly participating in signal transduction

pathways or by a general regulation of chromatin structure affecting gene expression.

We thank L. Ambrosio, C. Coffman, and members of the laboratory for discussion, advice, and critical reading of the manuscript. We also wish to acknowledge V. Lephart for maintenance of fly stocks. We thank V. Finnerty, A. Hilliker, A. Shearn, K. Dobie, and G. Karpen for generously providing fly stocks. This work was supported by National Institutes of Health grant GM-62916 (K.M.J.), by a Fung graduate award (Y. Jin), and by Stadler graduate fellowship awards (W.Z. and Y. Jin).

LITERATURE CITED

Beisel, C., A. Imhof, J. Greene, E. Kremmer and F. Sauer, 2002 Histone methylation by the *Drosophila* epigenetic transcriptional regulator *Ash1*. Nature **419:** 857–862.

Bellotto, M., D. Bopp, K. A. Senti, R. Burke, P. Deak *et al.*, 2002 Maternal-effect loci involved in *Drosophila* oogenesis and embryogenesis: P element-induced mutations on the third chromosome. Int. J. Dev. Biol. **46:** 149–157.

Campbell, S. D., A. Hilliker and J. P. Phillips, 1986 Cytogenetic analysis of the cSOD microregion in *Drosophila melanogaster*. Genetics **112:** 205–215.

Cavarec, L., S. Jensen, J-F. Casella, S. A. Cristescu and T. Heidmann, 1997 Molecular cloning and characterization of a transcription factor for the *copia* retrotransposon with homology to the BTB-containing *lola* neurogenic factor. Mol. Cell. Biol. **17:** 482–494.

Crosby, M. A., and E. M. Meyerowitz, 1986 Lethal mutations flanking the 68C *glue* gene cluster on chromosome 3 of *Drosophila melanogaster*. Genetics **112:** 785–802.

Crowner, D., K. Madden, S. Goeke and E. Giniger, 2002 *Lola* regulates midline crossing of CNS axons in *Drosophila*. Development **129:** 1317–1325.

Czermin, B., R. Melfi, D. McCabe, V. Seitz, A. Imhof *et al.*, 2002 *Drosophila* enhancer of Zeste/ESC complexes have a histone H3 methyltransferase activity that marks chromosomal Polycomb sites. Cell **111:** 185–196.

Dalby, K. N., N. Morrice, F. B. Caudwell, J. Avruch and P. Cohen, 1998 Identification of regulatory phosphorylation sites in mitogen-activated protein kinase (MAPK)-activated protein kinase-1a/p90rsk that are inducible by MAPK. J. Biol. Chem. **273:** 1496–1505.

Dingwall, A. K., S. J. Beek, C. M. Mccallum, J. W. Tamkun, G. V. Kalpana *et al.*, 1995 The *Drosophila snr1* and *brm* proteins are related to yeast SWI/SNF proteins and are components of a large protein complex. Mol. Biol. Cell **6:** 777–791.

Dobie, K. W., C. D. Kennedy, V. M. Velasco, T. L. McGrath, J. Weko *et al.*, 2001 Identification of chromosome inheritance modifiers in *Drosophila melanogaster*. Genetics **157:** 1623–1637.

Frodin, M., and S. Gammeltoft, 1999 Role and regulation of 90 kDa ribosomal S6 kinase (RSK) in signal transduction. Mol. Cell. Endocrinol. **151:** 65–77.

Giniger, E., K. Tietje, L. Y. Jan and Y. N. Jan, 1994 *Lola* encodes a putative transcription factor required for axon growth and guidance in *Drosophila*. Development **120:** 1385–1398.

Girton, J. R., and S. H. Jeon, 1994 Novel embryonic and adult homeotic phenotypes are produced by *pleiohomeotic* mutations in *Drosophila* Dev. Biol. **161:** 393–407.

Hardie, G., and S. Hanks, 1996 *The Protein Kinase Facts Book*. Academic Press, San Diego.

Ingham, P. W., and R. Whittle, 1980 *Trithorax*: a new homeotic mutation of *Drosophila melanogaster* causing transformation of abdominal and thoracic imaginal segments. I. Putative role during embryogenesis. Mol. Gen. Genet. **179:** 607–614.

Ishii, K., and U. K. Laemmli, 2003 Structural and dynamic functions establish chromatin domains. Mol. Cell **11:** 237–248.

Jin, Y., Y. Wang, D. L. Walker, H. Dong, C. Conley *et al.*, 1999 JIL-1: a novel chromosomal tandem kinase implicated in transcriptional regulation in *Drosophila*. Mol. Cell **4:** 129–135.

Jin, Y., Y. Wang, J. Johansen and K. M. Johansen, 2000 JIL-1, a chromosomal kinase implicated in regulation of chromatin structure, associates with the male specific lethal (MSL) dosage compensation complex. J. Cell Biol. **149:** 1005–1010.

Johansen, K. M., J. Johansen, Y. Jin, D. L. Walker, D. Wang *et al.*, 1999 Chromatin structure and nuclear remodeling. Crit. Rev. Eukaryot. Gene Expr. **9:** 267–277.

Lindsley, D. L., and G. G. Zimm, 1992 *The Genome of Drosophila melanogaster*. Academic Press, New York.

Mahowald, A. P., and M. P. Kambysellis, 1980 Oogenesis, pp. 141–209 in *The Genetics and Biology of Drosophila*, Vol. 2, edited by M. Ashburner and T. R. F. Wright. Academic Press, New York.

Makunin, I. V., E. I. Volkova, E. S. Belyaeva, E. N. Nabirochkina, V. Pirrotta *et al.*, 2002 The Drosophila suppressor of underreplication protein binds to late-replicating regions of polytene chromosomes. Genetics **160:** 1023–1034.

Meller, V. H., and M. I. Kuroda, 2002 Sex and the single chromosome. Adv. Genet. **46:** 1–24.

Muller, J., and M. Bienz, 1992 Sharp anterior boundary of homeotic gene expression conferred by the fushi tarazu protein. EMBO J. **11:** 3653–3661.

Muller, J., C. M. Hart, N. J. Francis, M. L. Vargas, A. Sengupta *et al.*, 2002 Histone methyltransferase activity of a *Drosophila* Polycomb group repressor complex. Cell **111:** 197–208.

Orlando, V., and R. Paro, 1995 Chromatin multiprotein complexes involved in the maintenance of transcription patterns. Curr. Opin. Genet. Dev. **5:** 174–179.

Papoulas, O., S. J. Beek, S. L. Moseley, C. M. McCallum, M. Sarte *et al.*, 1998 The *Drosophila* trithorax group proteins BRM, ASH1 and ASH2 are subunits of distinct protein complexes. Development **125:** 3955–3966.

Paro, R., 1990 Imprinting a determined state into the chromatin of *Drosophila*. Trends Genet. **6:** 416–421.

Pirrotta, V., and L. Rastelli, 1994 White gene expression, repressive chromatin domains and homeotic gene regulation in *Drosophila*. BioEssays **16:** 549–556.

Preston, C. R., and W. R. Engels, 1996 *P*-element-induced male recombination and gene conversion in Drosophila. Genetics **144:** 1611–1622.

Qian, S., M. Capovilla and V. Pirrotta, 1991 The bx region enhancer, a distant cis-control element of the *Drosophila Ubx* gene and its regulation by *hunchback* and other segmentation genes. EMBO J. **10:** 1415–1425.

Roberts, D. B., 1998 *Drosophila: A Practical Approach*. IRL Press, Oxford.

Rørth, P., K. Szabo, A. Bailey, T. Laverty, J. Rehm *et al.*, 1998 Systematic gain-of-function genetics in *Drosophila*. Development **125:** 1049–1057.

Rudenko, A., D. Bennett and L. Alphey, 2003 Trithorax interacts with type 1 serine/threonine protein phosphatase in *Drosophila*. EMBO Rep. **4:** 59–63.

Schüpbach, T., and E. Wieschaus, 1991 Female sterile mutations on the second chromosome of *Drosophila melanogaster*. II. Mutations blocking oogenesis or altering egg morphology. Genetics **129:** 1119–1136.

Shearn, A., 1989 The *ash1*, *ash2*, and *trithorax* genes of *Drosophila melanogaster* are functionally related. Genetics **121:** 517–525.

Shearn, A., T. Rice, A. Garen and W. Gehring, 1971 Imaginal disc abnormalities in lethal mutants of *Drosophila*. Proc. Natl. Acad. Sci. USA **68:** 2594–2598.

Shimell, M. J., J. Simon, W. Bender, and M. B. O'Connor, 1994 Enhancer point mutation results in a homeotic transformation in *Drosophila*. Science **264:** 968–971.

Simon, J., 1995 Locking in stable states of gene expression: transcriptional control during *Drosophila* development. Curr. Opin. Cell Biol. **7:** 376–385.

Simon, J., M. Peifer, W. Bender and M. O'Connor, 1990 Regulatory elements of the bithorax complex that control expression along the anterior-posterior axis. EMBO J. **9:** 3945–3956.

Smith, E. R., A. Pannuti, W. Gu, A. Seurnagel, R. G. Cook *et al.*, 2000 The *Drosophila* MSL complex acetylates histone H4 at lysine 16, a chromatin modification linked to dosage compensation. Mol. Cell. Biol. **20:** 312–318.

Spradling, A. C., M. deCuevas, D. Drummond-Barbosa, L. Keyes, M. Lilly *et al.*, 1997 The *Drosophila* germarium: stem cells, germ line cysts, and oocytes. Cold Spring Harbor Symp. Quant. Biol. **62:** 25–34.

Staveley, B. E., A. Hilliker and J. P. Phillips, 1991 Genetic organi-

zation of the cSOD microregion of *Drosophila melanogaster*. Genome **34:** 279–282.

Sullivan, W., M. Ashburner and R. S. Hawley, 2000 *Drosophila Protocols*. Cold Spring Harbor Laboratory Press, Cold Spring Harbor, NY.

Tamkun, J. W., R. Deuring, M. P. Scott, M. Kissinger, A. M. Pattatucci *et al.*, 1992 *Brahma*: a regulator of *Drosophila* homeotic genes structurally related to the yeast transcriptional activator SNF2/SWI2. Cell **68:** 561–572.

Wang, Y., W. Zhang, Y. Jin, J. Johansen and K. M. Johansen, 2001 The JIL-1 tandem kinase mediates histone H3 phosphorylation and is required for maintenance of chromatin structure in *Drosophila*. Cell **105:** 433–443.

Zhang, W., Y. Wang, J. Long, J. Girton, J. Johansen *et al.*, 2003 A developmentally regulated splice variant from the complex *lola* locus encoding multiple different zinc-finger domain proteins interacts with the chromosomal kinase JIL-1. J. Biol. Chem. **278:** 11696–11704.

Communicating editor: T. Schüpbach